The Centre for Australian Weather and Climate Research

A partnership between CSIRO and the Bureau of Meteorology

Australian Government

Bureau of Meteorology

CSIRO

Assessing the performance of a prognostic and a diagnostic cloud scheme using single column model simulations of TWP-ICE

Charmaine Franklin, Martin Dix, Christian Jakob and Greg Roff

CAWCR Technical Report No. 018

May 2009

www.cawcr.gov.au

Assessing the performance of a prognostic and a diagnostic cloud scheme using single column model simulations of TWP-ICE

Charmaine Franklin, Martin Dix, Christian Jakob and Greg Roff

CAWCR Technical Report No. 018

May 2009

ISSN: 1836-019X

National Library of Australia Cataloguing-in-Publication entry

Author: Franklin, Charmaine
Title: Assessing the performance of a prognostic and a diagnostic cloud scheme using single column model simulations of TWP-ICE / Charmaine Franklin, Martin Dix, Christian Jakob, Greg Roff
ISBN: 9781921605482 (pdf)
Series: CAWCR technical report ; no. 018
Notes: Bibliography
Subjects: Atmospheric circulation – Mathematical Models
Clouds – Mathematical Models
Other Authors/Contributors: Dix, Martin
Jakob, Christian
Roff, Greg
Dewey Number: 551.576

Enquiries should be addressed to:
Dr Charmaine Franklin
Centre for Australian Weather and Climate Research
A partnership between CSIRO and the Australian Bureau of Meteorology
Private Bag No. 1
Aspendale VIC 3195
AUSTRALIA
charmaine.franklin@csiro.au

Copyright and Disclaimer

Important Disclaimer

Contents

List of Figures

ABSTRACT

C. Franklin[1], M. Dix[1], C. Jakob[2] and G. Roff[1]

[1]*The Centre for Australian Weather and Climate Research*
[2]*School of Mathematical Sciences, Monash University*

Single column model (SCM) simulations using the UK Met Office Unified Model (UM), which is the atmospheric model in the Australian Community Climate Earth System Simulator (ACCESS), are presented for the Tropical Warm Pool International Cloud Experiment (TWP-ICE) field study. The formulations for the representation of clouds are compared to the extensive observations taken during the field campaign, giving insight into the ability of the model to simulate tropical cloud systems. Temperature and moisture fields as well as the vertical distribution of cloud properties are evaluated for a prognostic and a diagnostic cloud scheme. It is important in climate simulations to have the correct vertical distribution of clouds because clouds redistribute energy vertically and this distribution of energy affects both local and large-scale dynamics. The ACCESS/UM SCM produces the general cloud features observed during TWP-ICE. During the active monsoon period the model produces too much and deeper clouds and consequently the outgoing longwave radiation is too low. The thinner anvil cloud in the model runs during the suppressed phase results in too little longwave cooling and a subsequent warm bias in the upper troposphere. The monsoon break period is a difficult phase for the SCM to simulate and the resulting clouds are not as deep as those observed and too persistent. The prognostic cloud scheme is able to represent more of the observed variability of cloud properties and due to the differences in the way that the cloud schemes interact with convection, the prognostic scheme produces greater cloud amounts at the mid to high levels than the diagnostic scheme. Changing the shape of the vapour distribution in the model from a top-hat to a triangular distribution significantly reduced the low cloud cover, which lead to better agreement with observations, but did not impact the clouds in the upper troposphere due to the different forcing mechanisms for these clouds. The use of a cloud area fraction parameterisation that was developed for frontal clouds overestimates the cloud coverage when used for this tropical case, however, a sensitivity experiment shows that there is a need in the model to apply a cloud area fraction scheme to account for the model clouds not filling the grid box in the vertical.

1. INTRODUCTION

The Tropical Warm Pool International Cloud Experiment (TWP-ICE) was a major field campaign held in the Darwin area in January and February 2006. One of the main aims of the experiment was to provide boundary conditions and validation data for modelling studies to help facilitate model development with a focus on tropical convection and clouds. For a detailed report on the TWP-ICE campaign, including the meteorology and the observational network, see May et al. (2008). The Darwin area experiences a wide array of convective systems consisting of active monsoon periods with typical maritime storms and break periods with more coastal and continental convection. The observations collected during the TWP-ICE campaign allow for a detailed evaluation of the ability of numerical models to simulate the evolution of tropical cloud systems and their effect on the environment. Global climate models (GCMs) must be able to represent cloud-scale processes and the feedbacks between clouds and the large-scale environment to ensure accurate projections of climate change. One of the aims of this study is to examine the different effects of the diagnostic and prognostic cloud schemes on the state variables of temperature and humidity.

A useful tool in the evaluation and development of atmospheric physical parameterisations in numerical models are single column models (SCM) (e.g. Randall et al. 1996). The SCM represents a vertical column in a GCM and calculates the temporal evolution of the vertical profiles of temperature and moisture. The advection by the large scale flow is prescribed and the errors produced by the model's physical parameterisations will be reflected in the temperature and moisture fields. An advantage of the SCM approach is that by keeping the large scale atmospheric circulation fixed, a better assessment of the physical parameterisations on the local model state is enabled. SCMs provide a simple, inexpensive means to identify parameterisation errors and inadequacies, however, care needs to be taken in the interpretation of the SCM evaluation as the errors seen in the SCM may not be the same as those in the full three-dimensional GCM due to the lack of feedbacks between the physics and the dynamics in the SCM. If the SCM forcing data is realistic then the SCM may produce smaller biases than the GCM, however, because there is no feedback to the larger scales in the SCM simulation, the biases could grow with time and become larger than those of the full GCM (see e.g., Bergman and Sardeshmukh 2003).

The focus of this study is to evaluate the performance of the atmospheric model in tropical conditions associated with the monsoon and to identify areas for improvement in the model cloud and convection schemes. The Met Office has developed a new generation prognostic cloud scheme (Wilson et al. 2008a) and the model evaluation presented in this work provides a comparison of the new cloud scheme with the control diagnostic scheme. The results presented in this study build on the work of Wilson et al. (2008b) where climate runs with the two UM cloud schemes were compared against each other and observations. This SCM study is the first to use the TWP-ICE forcing and evaluation dataset and as such provides insights into the usefulness of the data for model evaluation. The next section will describe the model and the forcing and validation data used in this study. Section 3 describes the general characteristics of the TWP-ICE meteorology and discusses the model performance for the three weather regimes that occurred during the campaign, with a focus on the temperature and moisture budgets and the differences between the prognostic and diagnostic cloud schemes. Section 4 compares the variability of the cloud properties simulated by the prognostic and diagnostic cloud schemes and this is followed by a summary of the findings of this study in section 5 and a discussion of the parameterisation inadequacies identified.

2. EXPERIMENT DESIGN

The Australian Community Climate Earth System Simulator (ACCESS) is a new coupled climate and earth system model that is being developed as a joint initiative between the Australian Bureau of Meteorology and CSIRO in partnership with Australian universities. The model provides a framework for numerical weather prediction and studies of climate change and enables research into processes occurring in the earth system (for information on the modelling system see http://www.accessimulator.org.au/). The atmospheric component of ACCESS is the UK Met Office Unified Model (UM) and throughout this paper the model with be referred to as the ACCESS model. As part of the ACCESS project this model needs to be extensively validated in the Australian region. One of the experiments designed to evaluate the ACCESS atmospheric model in the Australian region is to run the SCM for the TWP-ICE case. This recent intensive field campaign has produced a new data set for model evaluation and as such is an ideal case study for the ACCESS model.

2.1 Description of the ACCESS/UM single column model

The ACCESS SCM used in this study is the UM version 6.3 with 38 vertical levels, which includes:

- vertical advection, which is described by the semi-Lagrangian scheme of Davies et al. (2005);
- atmospheric longwave and shortwave radiation modelled by the Edwards and Slingo (1996) scheme, which allows for the effects of water vapour and clouds that are maximal-randomly overlapped;
- large-scale precipitation determined from the water or ice content of a cloud and described by Wilson and Ballard (1999);
- turbulent transport within the boundary layer as described by Lock et al. (2000) for the total specific humidity (vapour plus liquid) and by Roe (1985) for the cloud ice water content;
- convection based on the Gregory and Rowntree (1990) scheme, which is built on the initial buoyancy flux of a parcel of air and includes entrainment, detrainment and the evaporation of falling precipitation;
- large-scale cloud as described by either the diagnostic scheme of Smith (1990) with modifications (Wilson et al. 2004) or the new Met Office prognostic cloud scheme PC2 (Wilson and Bushell 2007; Wilson et al. 2008a), note that the ice condensate is prognostic in both schemes.

The new prognostic cloud scheme that has been developed for the UM includes prognostic variables for the cloud liquid water content, the cloud ice water content, the bulk cloud fraction, the liquid cloud fraction and the ice cloud fraction (for a detailed description see Wilson and Bushell (2007) and Wilson et al. (2008a)). Diagnostic cloud schemes such as the Smith (1990) scheme are relatively simple in their representation of cloud properties and exhibit strongly constrained relationships between cloud variables. These relationships restrict the variability of the cloud fields and can produce unrealistic cloud properties (Wilson et al. 2008a). The new cloud scheme PC2 (prognostic cloud prognostic condensate) was designed to be more realistic by allowing a greater number of degrees of freedom in the cloud variables to overcome some of the difficulties of the Smith (1990) scheme. Another advantage of a fully prognostic cloud scheme is the memory of the cloud fields that exists between model time steps. In a diagnostic scheme the lack of any knowledge of whether cloud existed at a previous time step can result in unrealistic intermittent cloud fields. PC2 is similar to the Tiedtke cloud scheme (Tiedtke 1993) in that increments to the cloud fields are considered from each physical and dynamical process in the model. However, PC2 differs from the Tiedtke (1993) scheme in its formulation of the source and sink terms, the numerical implementation of the cloud scheme and the distinction between the liquid and ice phases. Representing changes in the prognostic cloud variables from each physical process in the model allows a way to directly link the cloud condensate and cloud fraction together and consistently simulate the effects of physical processes in a much more complete and realistic way than a diagnostic scheme (Wilson et al. 2008a).

The ACCESS atmospheric model has two changes made to the parameterisation of the convective updrafts when the PC2 scheme is used. The first is an increase in the proportion of condensate that is detrained high in the convective plumes, rather than being precipitated. The second change is a reduction of the phase-change temperature between liquid and ice condensate in the convective updrafts. In the PC2 simulation this temperature is reduced from the control value of 0°C to -10°C. These changes are necessary to produce realistic anvil clouds due to the direct interaction of the large-scale cloud variables in PC2 with the convection scheme (see Wilson et al. 2008b for more details on these changes).

2.2 The TWP-ICE forcing and validation data

The large-scale single-column model forcing and evaluation data set was derived from the constrained variational objective analysis approach described in Zhang and Lin (1997) and Zhang et al. (2001) using the observations taken during TWP-ICE (Xie et al. 2007). The aim of the objective analysis is to make minimum adjustments to the original sounding data to constrain the wind, temperature and humidity fields to satisfy conservation of mass, moisture, energy and momentum through a variational technique. The constraint variables used are surface pressure, surface latent and sensible heat fluxes, wind stress, precipitation, net radiation at the surface and top of the atmosphere, and variability of total column water content. The method takes into account measurement uncertainties and it has been shown that the magnitude of the adjustments required to meet conservation is comparable to these uncertainties (Zhang and Lin 1997).

The domain used in the objective analysis is pictured in Figure 1 in May et al. (2008) and covers an area of roughly 150 km radius centred on Darwin. Within this area there were five boundary sounding stations that measured the vertical profiles of temperature, relative humidity and winds every 3 hours during the intensive observation period. At the ARM Darwin site, which is at the centre of the analysis domain, soundings were available 4 times a day. These original soundings had a dry bias that has been corrected by Hume (2007) who applied a radiation dry bias correction factor, a temperature dependent calibration correction factor and a solar zenith angle correction factor. The ratios of missing data to the total data range from 5 to 30% for the 5 boundary sounding sites, with the largest amount of missing data occurring for the soundings taken from the ship (Xie et al. 2007). The variational analysis also required domain-averaged surface and top of the atmosphere measurements and these were provided by the Australian Bureau of Meteorology precipitation radar data, surface radiative and turbulence fluxes from the ship and land stations, surface meteorological fields from both the local mesonet and sounding stations, cloud liquid water path from the ARM site and the ship, and satellite data from the Multi-functional Transport Satellite (MT-SAT). Any missing observations that the variational analysis needed were provided by the ECMWF model data, where the ECMWF data were adjusted using the linear regression equations that were derived at times when observations were available (Xie et al. 2007). For further details on the data sources see http://science.arm.gov/wg/cpm/scm/scmic6/forcing_data.html.

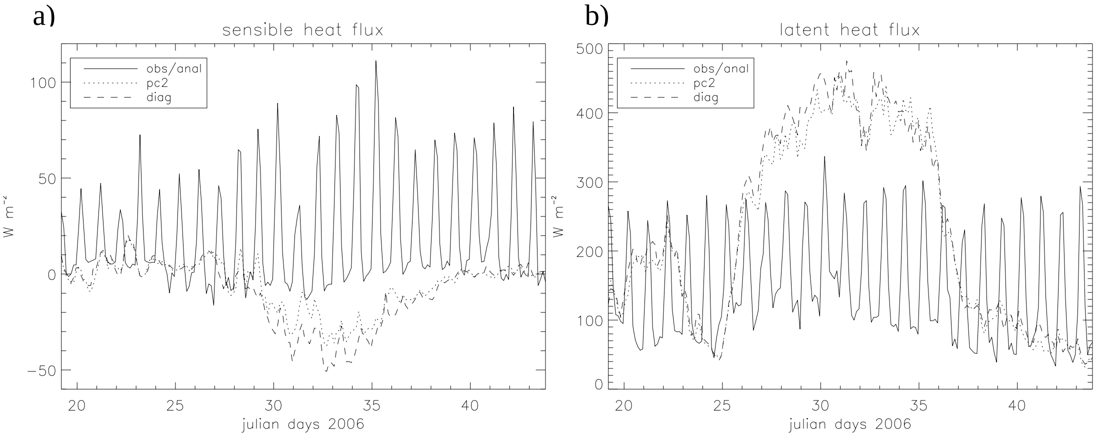

Figure 1: a) Surface sensible and b) latent heat fluxes (W m^{-2}) averaged over the TWP-ICE domain as given by the observations/analysis and the SCM runs with the PC2 and diagnostic cloud scheme.

The observational forcing dataset has a temporal resolution of 3 hours and the data needed to force the SCM has been linearly interpolated to 30 minutes, which is the timestep used in the SCM simulations. The model is initialised once on 19 January 2006 and then run for 25 days. The lower boundary condition used in the SCM experiments is a prescribed sea surface temperature (SST), where the model then calculates the turbulent fluxes of sensible and latent heat at the surface rather than forcing the model fluxes to be those that have been observed. The reason for this choice is due to the significant amount of missing data for the surface flux measurements, with some periods lasting more than a week (Xie et al. 2007). Given that the domain consists of both land and sea, using the prescribed SST means that the experiment is slightly less realistic, and limits the results in not being able to study the diurnal cycle as the resulting surface fluxes do not have the correct magnitude in their fluctuations across the day (Figure 1). This methodology has also been adopted in cloud resolving modelling of TWP-ICE (Fridlind et al. 2008). Three-dimensional advective tendencies are specified as forcing from the variational objective analysis and the model horizontal wind fields are relaxed back to those from the observations over 3 hour periods. Cloud amount and cover in the model is initialised from the temperature, moisture and pressure fields and these fields are not advected throughout the simulation since these quantities are not measured. We chose not to nudge the temperature and moisture fields for two reasons: nudging can mask errors from the model physics that affect temperature and humidity (Ghan et al. 1999), and nudging these fields can also change cloud morphology through the elimination of radiative feedbacks on cloud formation (Menon et al. 2003). As one of the aims of this study is to examine the different effects of the diagnostic and prognostic cloud schemes on the state variables of temperature and humidity, nudging these variables was deemed unsuitable.

3. MODEL EVALUATION

In the analysis presented in this section the observations that are used to examine model performance and compare cloud schemes are derived from various sources including i) the objective analysis that was described in the previous section, ii) the raw data that is available from the ARM facility in Darwin, and iii) data products derived from satellite, radar and lidar data for the ice water path and cloud fraction. As discussed previously the adjustments made to the temperature and humidity sounding data through the objective analysis procedure are of the same magnitude as the observational uncertainties of these quantities (Zhang and Lin 1997). This means that the evaluation data for these fields have had minimum adjustments made to bring them into balance with the advective forcings and the column integrated budgets of mass, moisture, energy and momentum, which ensures a dynamically and thermodynamically consistent dataset. This dataset can be used to drive and evaluate SCMs and to perform budget studies. The evaluation data from the objective analysis are denoted as obs/anal in the figures and where an observation other than that from the analysis is used, details about that data are provided in the corresponding discussion of the model results.

The SCM forcing data, which provides the tendencies due to the large-scale forcing of potential temperature, specific humidity, horizontal and vertical winds, are derived using the surface precipitation rate as one of the fields that constrain the heat and moisture budgets. Because of this, the use of the precipitation observations to validate model performance is generally not meaningful, however, it is shown in Figure 2a to validate the experiment set up by the agreement between the observations and the model predictions of surface rainfall and to illustrate the different meteorological regimes that occurred throughout TWP-ICE. As discussed by May et al. (2008), initially TWP-ICE was characterised by an active monsoon period from January 19 – January 24. The strong forcing associated with the deep convection during this time produces average rainfall rates of 17 mm/day (see Fig. 2a) and there is little deviation between the observations and the model results. As the meteorological regime shifts to a suppressed monsoon phase both runs produce more precipitation than the observations. The difference between the modelled and the observed precipitation rates is evident from January 25 until February 5. After this time the precipitation rates of the SCMs tend to agree with those observed and Figure 2a shows that the differences in the cumulative precipitation remain fairly constant over this last period, which is characterised by more continental and coastal convection generated from sea breezes in this break period. The two SCM runs differ only in their large-scale cloud scheme and Figure 2a shows that the difference in the total surface rainfall rate between the two runs is small.

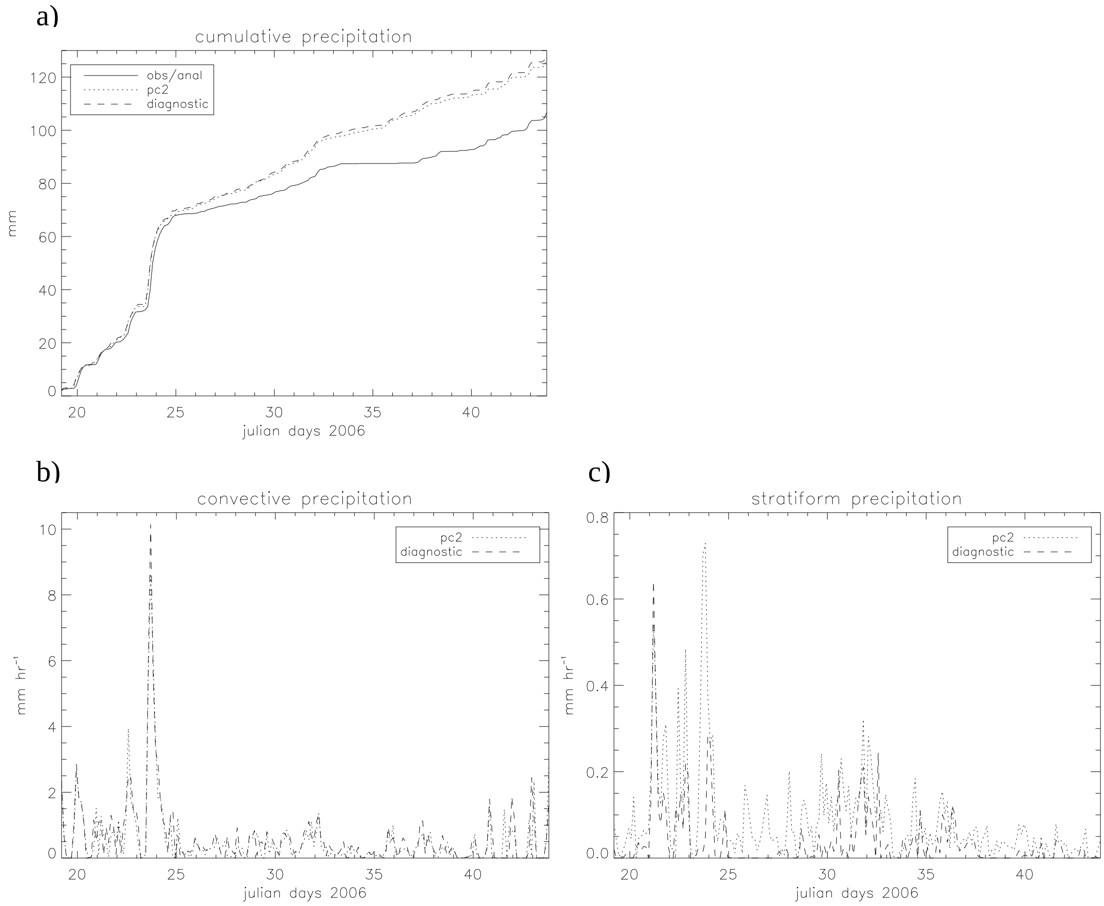

Figure 2: a) Cumulative surface rainfall (mm) averaged over the TWP-ICE domain as given by the observations and the SCM runs with the PC2 and diagnostic large-scale cloud schemes. b) Convective precipitation rates (mm hr^{-1}) from the model runs, rates are taken from the 3 hourly averaged data. c) as for b) except for the stratiform or large-scale precipitation rates.

A break down of the total observed surface rainfall into convective and stratiform components is yet to be undertaken for TWP-ICE, however, it seems likely that the convective proportion will be typical of tropical cloud systems in which 60-70% of the rainfall is convective and 30-40% arises from stratiform rain processes. The two large-scale cloud schemes use the same cloud microphysics scheme and the differences that are shown in the partitioning of the rainfall into convective and stratiform contributions shown in Figure 2b and 2c are due to the differences in the formulations of the large-scale cloud properties. PC2 shows a greater percentage of stratiform rain across the length of the simulation compared to the diagnostic scheme. The run with the PC2 scheme produces 14% of the rain through the stratiform cloud processes compared to only 5% from the diagnostic cloud scheme. This higher percentage of stratiform rain is expected since condensate detrained from convection becomes a direct source for the PC2 large-scale cloud scheme rather than evaporating into the environment before being processed by the diagnostic cloud scheme. While the higher percentage of stratiform rain from the PC2 run is more realistic, it is still only half of what is typically produced by stratiform clouds in the tropics. The associated heating profile from stratiform rain processes has been shown to play an important role in the representation of the Madden-Julian oscillation (MJO) (Lin et al. 2004) and although it is very difficult to directly compare the convective-stratiform partitioning of large-scale models to observations, if models are to produce the correct diabatic heating profiles a better partitioning of convective and stratiform rain processes could be key. One possible reason why the convective precipitation is excessive could be due to the microphysics within the convection scheme being too efficient. The microphysical processes represented in cumulus parameterisations tend to be much simpler than those in the stratiform cloud scheme and this could contribute to the unrealistic partitioning seen in the SCM precipitation rates. The convection scheme in the SCM converts all condensate above the fixed threshold of 1 g kg^{-1} or the local saturation specific humidity where it is less, directly into precipitation once the cloud depth reaches a critical value. Menon and Rotstayn (2006) found strong sensitivity to the treatment of convective condensate, with changes to the treatment of the threshold that governs precipitation amounts producing a larger influence on liquid water path than changes in aerosol distributions.

The two horizontal wind field components that were observed during TWP-ICE are shown in Figure 3. The errors in the predicted wind fields do not exceed 6 m s^{-1} as the winds are being relaxed to the observed winds every 3 hours. Figure 3a shows the zonal winds that were observed during TWP-ICE and characteristic of monsoon conditions the winds during the active and suppressed monsoon phases were generally westerlies between 700 and 850 hPa. On days 23 – 24 the winds averaged over the TWP-ICE domain in the low levels were easterlies due to the monsoon trough receding to the north of Darwin and it was at this time that a large mesoscale convective system developed into a tropical low. This system maintained strong low-level westerly winds until it dissipated on February 3 and the winds soon after changed to low-level easterlies that coincide with the break period. The meridional winds in Figure 3b show a tendency to be from the north except when the tropical low has developed, where the mid-level winds are mostly southerlies overlayed by strong northerlies between 14 and 18 km.

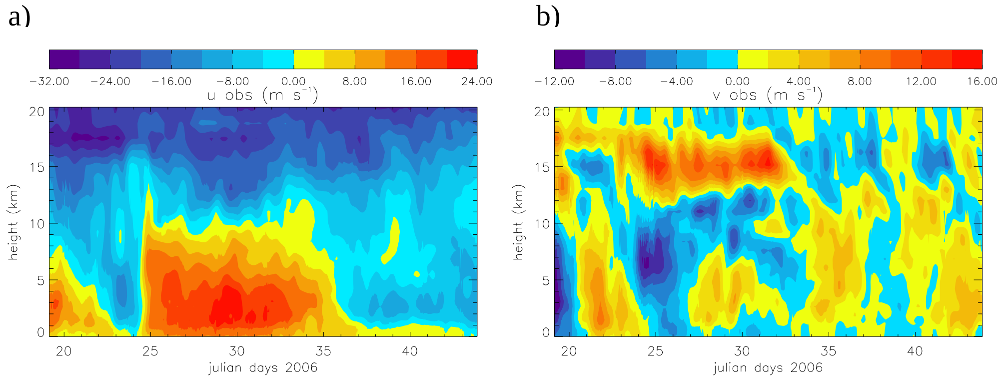

Figure 3: Three hourly observations of the a) u and b) v wind components (m s^{-1}).

3.1 The active monsoon period (Julian days 19 - 24)

The Darwin ARM site has a suite of active remote sensing instruments that provide vertical cloud structure information. The Active Remotely Sensed Cloud Layers (ARSCL) data has been provided as part of the TWP-ICE validation data set and gives information on the location of cloud layers (see Clothiaux et al. 2000 for details). Following Jakob et al. (2005) the 10s ARSCL data are converted into hydrometeor/cloud cover by counting the number of times there is cloud in a 100 m vertical layer of the atmosphere within an hour and then dividing by the number of observations taken during that hour. The observed cloud cover has been plotted in Figure 4 along with the cloud cover from the two model runs with differing cloud schemes. The observations show clearly the three meteorological regimes that were experienced through TWP-ICE. During the active monsoon phase of the experiment over days 19 to 24, deep clouds up to 17 km were observed on all days. This was followed by a period of suppressed convection that was initially characterised by cirrus and anvil cloud and then a few predominately clear days. After this time the regime shifted to a break period and the observed clouds reached heights of up to 15 km but were less persistent than those that occurred during the active period. The SCM runs both show reasonable agreement with the observations, however, there are notable biases and clear differences between the model cloud fields. The observations have a vertical resolution of 100 m that is much higher than that of the model, which is about 1km in the upper troposphere and thus there is some smearing out of the model cloud fields that is purely due to the limited model resolution. Initially the model cloud fields reach heights in excess of 18 km, which is about 3 km higher than the observations of Figure 4a. It should be noted that at these heights the radar's ability to detect small ice particles (Comstock et al. 2002) is limited and the observed cloud heights may be underestimated. This underestimation was aggravated for TWP-ICE due to a lightning strike at the Darwin ARM site that occurred before the experiment and resulted in a loss of radar sensitivity (May et al. 2008).

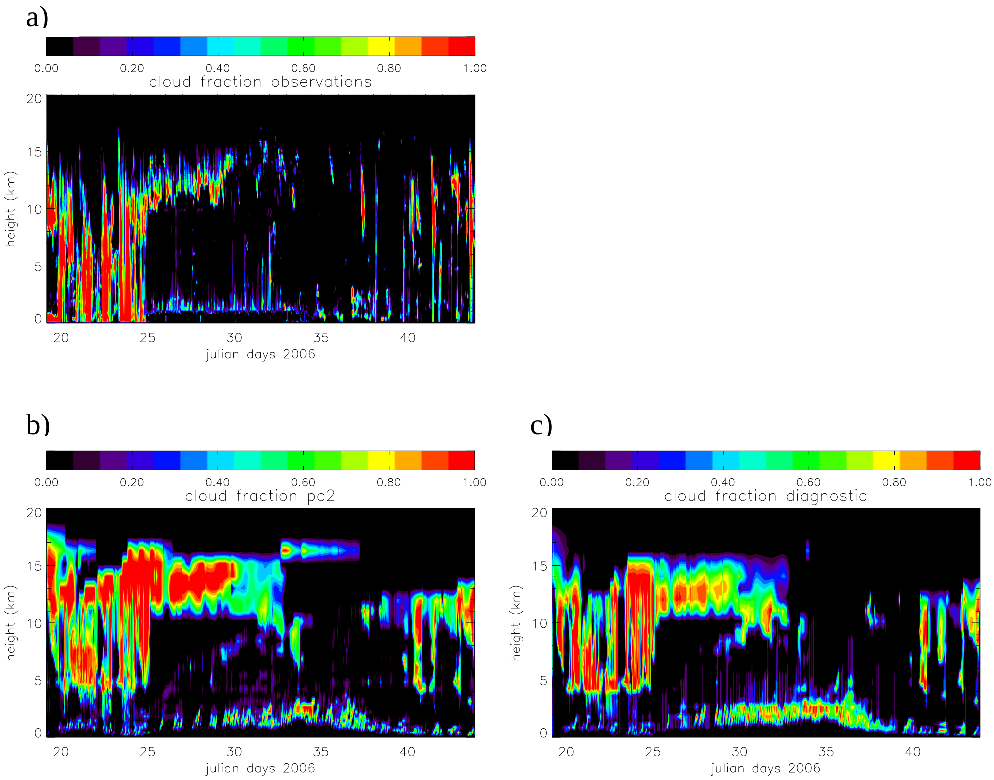

Figure 4: a) The observed cloud fraction or hydrometeor fraction. b) As for a) except for the SCM runs with the PC2 scheme. c) As for a) except for the SCM run with the diagnostic cloud scheme.

The SCM run with the prognostic cloud scheme tends to produce deeper clouds than the run with the diagnostic scheme over the active period and has a stronger diurnal signal in the cloud top heights over days 23 – 25 when a mesoscale convective system was present in the experiment domain. These differences are due to the way in which the prognostic and diagnostic cloud schemes interact with the cumulus parameterisation, which is discussed in detail in the following subsection. Radiation fields can be used to evaluate the combined effects of the cloud layers on the absorption and reflection of the solar and infra-red radiation. The SCM runs both use the assumption of a maximum-randomly distributed cloud field (i.e., maximum overlap of adjacent but random overlap of separate cloudy layers). Figure 5a shows the outgoing longwave radiation (OLR) at the top of the atmosphere for the observations that fit the budgets in the variational analysis, and the results for the SCM runs. Note that the "no acf" simulation results shown in Fig. 5 correspond to a sensitivity run that will be discussed in section 4. On average during the active period the PC2 simulation produces lower OLR than the diagnostic cloud scheme and the observations, consistent with an overestimation of deep clouds. Averaged over the active monsoon period the PC2 simulation produces higher liquid and ice cloud water contents than the diagnostic scheme run by 21 and 34% respectively. Figure 5b shows the downward solar radiation at the surface that was observed and modelled for TWP-ICE. On day 22 the SCM with PC2 shows a large overestimation of the incoming solar radiation at the surface, indicating that there was not enough cloud at this time to reflect the solar radiation, however the trend on the other days during the active period is for the models to under predict the incoming solar radiation at the surface in agreement with other observations indicating that the models produce too much cloud during this period.

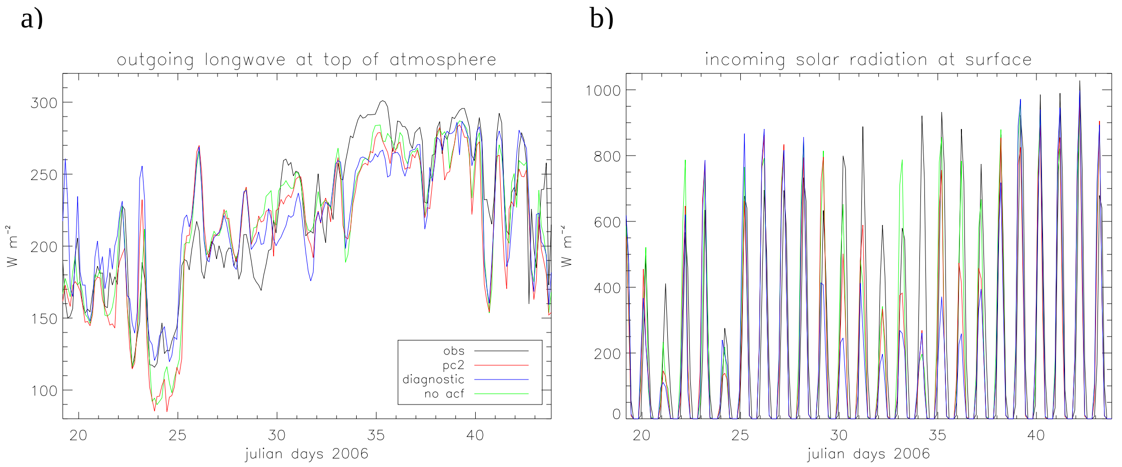

Figure 5: a) Observed and simulated outgoing longwave radiation at the top of the atmosphere (W m^{-2}). b) Observed and simulated incoming solar radiation at the surface (W m^{-2}).

The PC2 large scale cloud scheme calculates increments at every timestep to the temperature and water vapour fields from each of the dynamic and physical processes represented in the atmospheric model. Three hourly averaged temperature increments from each of the physical processes in the SCM and the observational forcing (the advective forcing) are shown in Figure 6. Averaged over the full run (Fig 6a) convection tends to warm the atmosphere, opposing the cooling from the large-scale processes. The stratiform rain, driven by the microphysics of the stratiform cloud component, acts to cool the atmosphere below the freezing level through evaporation and melting, and warm the levels above by condensation. Heating from shortwave radiation has a mostly uniform profile throughout the column and longwave cooling is maximal from about 5-13 km. The boundary layer transports warm air from the surface into the lowest levels of the atmosphere. The average heating profile for the different processes remains much the same for the active monsoon phase (Fig. 6b) except that the magnitudes of the terms increase substantially (note the different scale). The location of the freezing level is readily apparent in the convection and microphysics heating profiles. At this height the gradient of the convective heating rate changes and reflects the large effect of detrainment as the buoyant air reaches the more stable layer near the melting level at about 5 km. The budgets shown in Figs. 6c and 6d will be discussed in the following subsections.

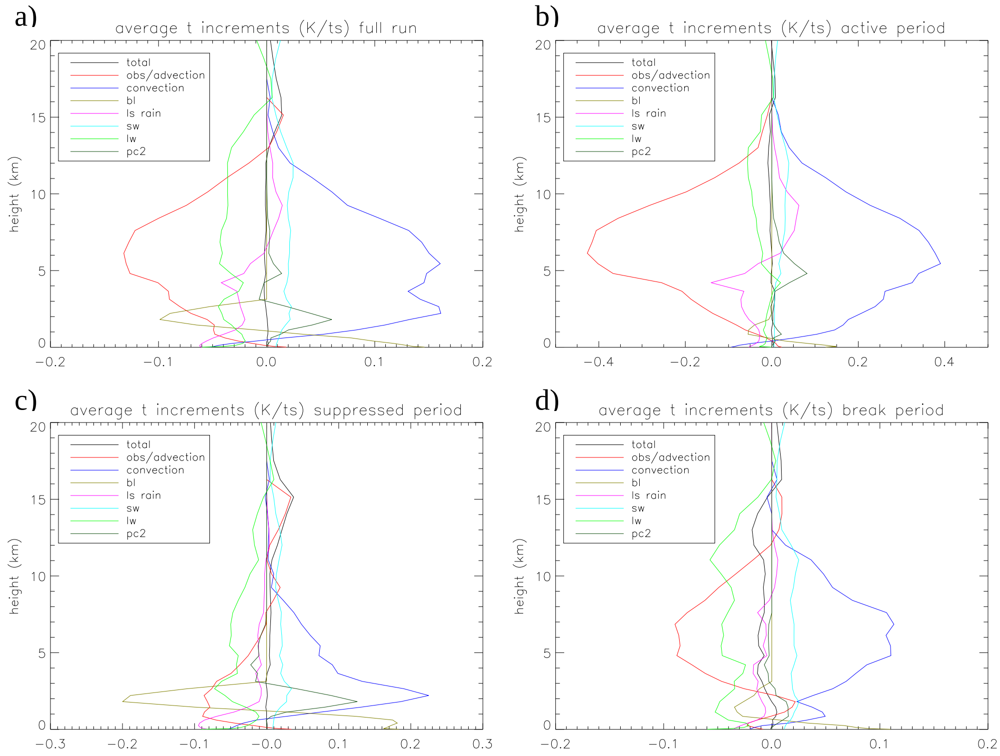

Figure 6: a) 3 hourly temperature increments (K timestep^{-1}) from the observations (advective tendencies), the convection, the boundary layer, the microphysics or large-scale rain, the shortwave and longwave radiation and the total increment. a) The average over all times, b) over the active monsoon period (days 19 – 24), c) over the suppressed monsoon period (days 25 – 35) and d) over the break period (days 36 – 44).

The bias in the modelled temperature fields are shown in Figure 7. This signal of a warm bias above and a cool bias below is not unusual in tropical SCM runs where the levels above the convective cloud tops are warmed due to the temperature forcing, which cannot be counterbalanced by the physical processes in the model (see e.g. Bechtold et al. 2000). In the tropics temperature fluctuations result from relatively small imbalances between the diabatic and adiabatic tendencies. In SCM runs the adiabatic tendencies are prescribed and this can decouple them from the diabatic tendencies resulting in larger temperature tendencies than those observed (Bergman and Sardeshmukh 2003). The location, timing and magnitude of the warm temperature bias in the upper troposphere shown in Fig. 7 are very similar to the bias shown when the forcing data is used to run a cloud resolving model (Jon Petch personal communication). As this is the first application of the TWP-ICE forcing dataset, there is also the possibility that a small error in the forcing data is accumulating throughout the length of the simulation to contribute to this bias. The bias does not change significantly when the SCM is initialised at different times throughout the run (Laura Davies personal communication). These results suggest that the upper tropospheric warm bias is a robust signal that is inherent in tropical SCM forcing data but is reinforced by the interaction with radiation and inadequacies in the model physics as will be discussed later. During the active period the peak of the cold bias occurs at the heights between 11 and 13 km where the cloud ice concentrations are maximal and there is a secondary peak in the cold bias just below 5 km associated with the melting level. Figure 6b shows the cold bias across these levels and the processes that are active during this period that contribute to this bias. The cold bias could be a result of not active enough convection or not enough condensational heating occurring from the large-scale cloud. However, given that the models tend to produce too much cloud at these times as supported by radiation measurements, it seems likely that the reason for the cold bias from 7-15 km is the excessive longwave cooling throughout the upper cloud levels. The secondary cold bias peak that is collocated with the melting level is probably caused by the strong cooling from the cloud microphysical processes of the stratiform cloud. At this level the melting of hydrometeors produces a sharp gradient in the cooling and the overestimation of cooling could be due to the larger ice cloud fraction in the simulation compared to the observations (as will be shown in section 4), which is used to calculate the wet-bulb temperature that partly governs the melting rate.

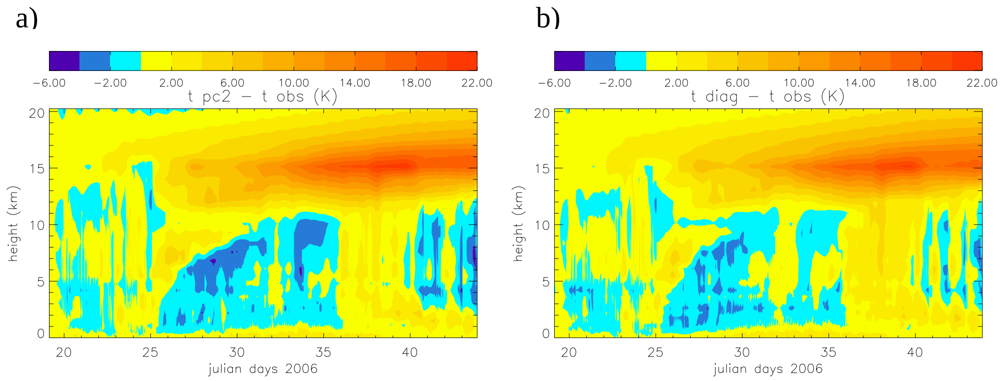

Figure 7: a) The difference between the temperature of the SCM with the PC2 cloud scheme and the observations (K). b) As for a) except for the SCM with the diagnostic cloud scheme.

Similar to the budget of the temperature increments shown in Figure 6, Fig. 8 shows the increments to the water vapour field. Averaged over the full simulation convection dries the atmospheric column and the magnitude of the drying opposes the moistening from the boundary layer in the lowest 2 km and the advective forcing above this height. The large scale rain or the microphysics acts as a source of water vapour through the process of evaporation below the melting level and a sink of water vapour above this level where the growth of hydrometeors through deposition depletes the atmospheric water vapour. Shortwave and longwave radiation change the temperature of the atmosphere and the associated condensation/evaporation is calculated within the model. The effect of this radiative forcing on the water vapour budget is small and the 3 hourly average changes in the water vapour content of the atmospheric column due to longwave and shortwave radiation cooling/heating are the smallest increments. The active monsoon period is characterised by much larger water vapour increments in the levels between 2 and 10 km (see Fig. 8b) compared to the average over all 3 periods. The convective increment in Figure 8b shows the large effect of detrainment as the buoyant air reaches the more stable layer near the melting level at about 5 km. The deep convection at these times is reflected in the significant sink of water vapour due to the growth of hydrometeors occurring between the freezing level up to above 10 km.

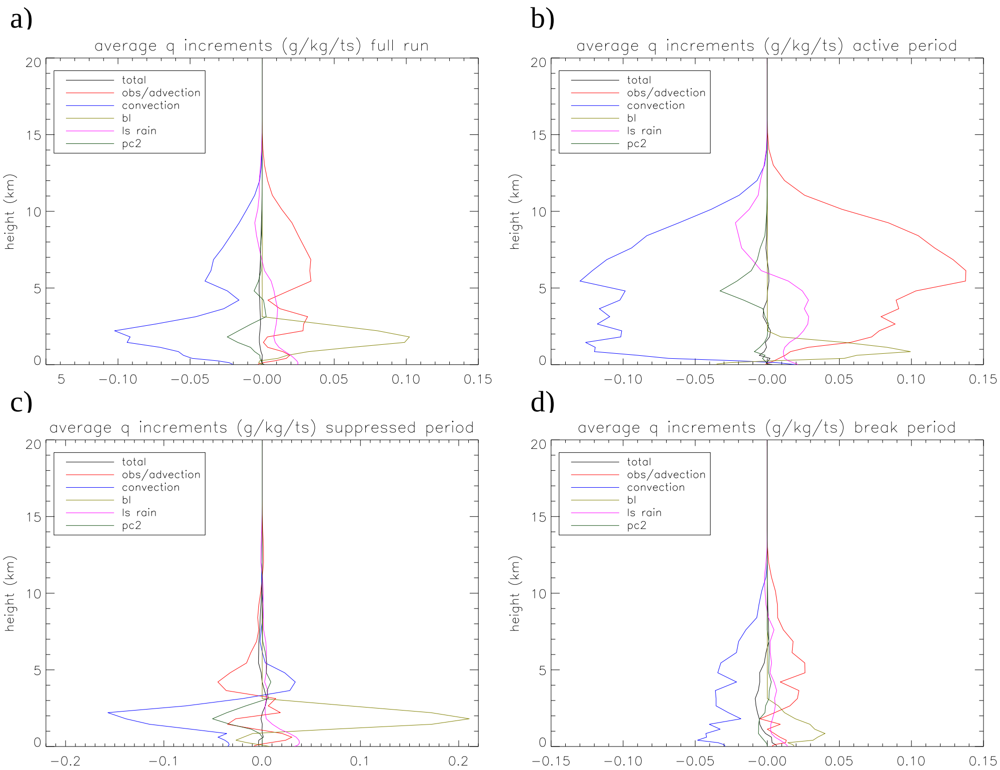

Figure 8: As in Figure 6 except for the 3 hourly averaged water vapour increments (g kg^{-1} timestep^{-1}).

Figure 9 shows the specific humidity observations below 10 km and the difference between the observations and the two SCM runs. Both of the models show the same error pattern: a tendency to be drier than the observations below 2km particularly during the suppressed monsoon phase where a strong dry bias extends to 6 km, a weak moist bias is present above about 3 km during the active period and a stronger moist bias exists below 5 km during the clear days of the transition period between the suppressed monsoon and the break periods. It should be noted that the large-scale humidity observations will probably have the largest uncertainty of all of the state variables (Zhang and Lin 1997). Errors associated with radiative heating of sensors have been corrected (Hume 2007) but there are still uncertainties due to the slow response of the humidity sensor when entering and exiting from cloudy regions and the possible contamination by ice (Zhang and Lin 1997). The detrainment from convective clouds just below the freezing level due to the enhanced stability of this layer moistens the atmosphere and leads to a small moist bias at these heights during the active monsoon phase. The average moisture biases are the weakest for the active monsoon period and there is essentially no difference between the runs with the differing cloud schemes. In this period the forcing is very strong and the models are so tightly constrained that they both produce the same response to the forcing. Figure 8b shows that the dry bias below 4 km in the active period could be a result of the convection being too efficient at drying these levels of the atmosphere or not enough evaporation occurring from the stratiform rain to moisten the atmosphere.

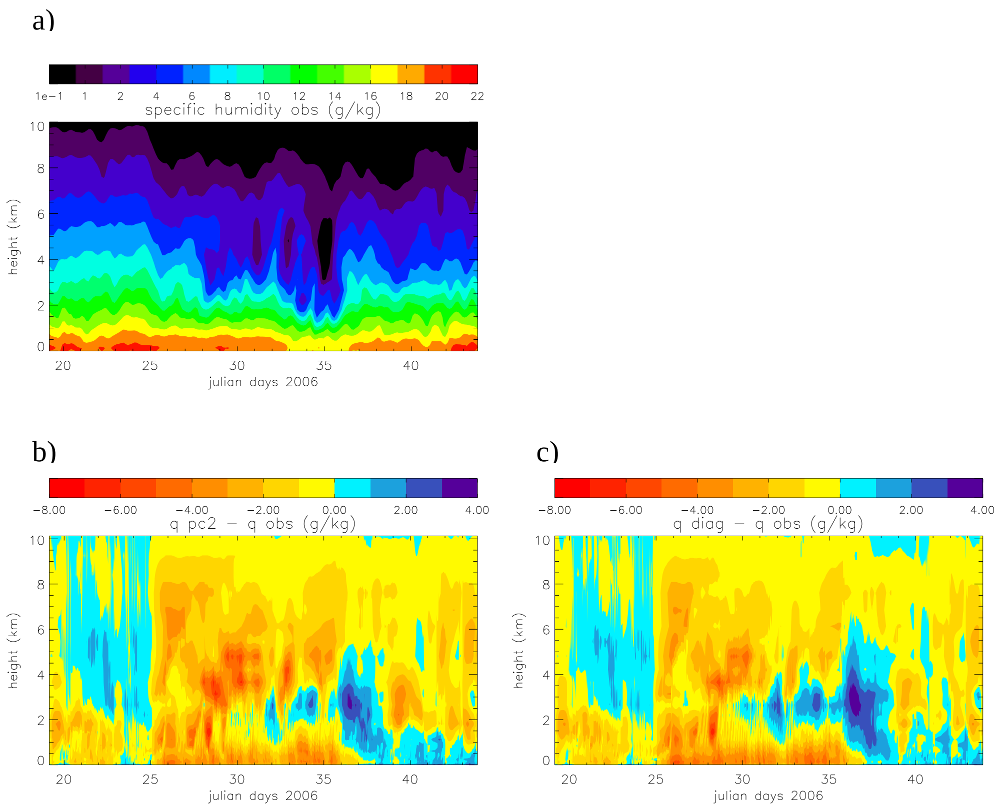

Figure 9: a) 3 hourly observations of the specific humidity (g kg^{-1}). b) The difference between the specific humidity of the SCM with the PC2 cloud scheme and the observations. c) As for b) except for the SCM with the diagnostic cloud scheme.

3.2 The suppressed monsoon period (Julian days 25 - 35)

During the suppressed monsoon period the cloud structure changed from being characterised by the deep convective clouds of the preceding active monsoon phase, to shallow and occasional midlevel convective clouds topped by an extensive high level cloud shield as shown in Figure 4a. The expansive high cloud in the PC2 run during the suppressed phase shows more vertical structure and less intermittency than that produced from the diagnostic scheme with no memory (see Fig. 4b and c). The ice clouds that consist of both cirrus and anvil outflow from deep convection show a decrease in maximum cloud cover with height. This feature is more notable in the observations than the SCM results and arises because of the settling of larger particles and possibly the decrease in water vapour with height. The diagnostic cloud scheme produces a better representation of the ice cloud cover vertical gradient than PC2; note that the ice condensate is a prognostic variable in both cloud schemes and that both simulations use the same microphysics parameterisations. The two simulations show too much midlevel cloud as compared to the observations during the suppressed phase of days 25 – 35, with the diagnostic cloud scheme producing greater midlevel cloud cover than the PC2 scheme. The erroneous high level cloud feature that occurs in this run on day 32 is sourced by the convection scheme, which generates saturation at 16 – 18 km and is due to the warm upper level temperature bias and the associated instability. Throughout the first 5 days of the suppressed phase the SCM runs reduce the cloud field too much compared with the radiation observations in Figure 5 and suggest that neither of the models produce a thick enough anvil. After this time the models fail to dissipate their high cloud as the observations show (see Fig. 4) and underestimate the period of high OLR (Fig. 5a).

The average temperature increments for the suppressed monsoon period are shown in Figure 6c. The warm bias that is present (Fig. 7a) in the levels above 12 km is clearly shown to be forced from the observation/advective temperature tendencies at these levels. The warming in this region coincides with the location of the cirrus and anvil clouds. The lack of a thick enough anvil cloud to offset this warming by longwave radiative cooling appears to be the main reason for the warm temperature bias at the levels between 11 and 16 km during this period. The cool bias below this level is likely to also be caused by the longwave radiation, but in this case there is too much cooling due to the excessive amount of midlevel cloud shown in both of the simulations (Figure 4b) and the lack of high clouds to trap outgoing longwave radiation.

The stronger cold temperature bias seen in the PC2 run for both the suppressed and break periods between the freezing level and 10 km could be due to the differences in the way that convection and the stratiform cloud scheme interact and the consequences of this on the strength of convection. In PC2 the convection scheme detrains condensate directly into the grid box thereby allowing the stratiform cloud scheme to reflect details of the convective clouds. This differs from the diagnostic scheme where the detrained condensate evaporates and the radiative effect of the convective cloud is represented by a separate diagnostic cloud category. The changes that have been made to the convection scheme for the PC2 model are the reduction of the temperature at which the phase-change occurs within the convective plume, which is important for the representation of supercooled water and parcel buoyancy (see Wilson et al. 2008a for a discussion), and the increase in the maximum amount of condensate that can be detrained rather than precipitated out of the convective updrafts. Wilson et al. (2008b) discuss the reasons for adjusting the convective precipitation function and demonstrate the effects of this change. They show that without tuning the detrainment of condensate in PC2 results in a drying of the upper tropical troposphere, leading to an environment that is not conducive to sustaining stratiform cloud. The result of this later change is that more condensate is detrained rather than precipitated out of the convective plume and this is demonstrated by the 67% increase in cloud ice water content in the PC2 simulation compared to the diagnostic scheme result for the suppressed period.

The water vapour budget during the suppressed monsoon period (see Figure 8c) shows that the drying due to convection tends to balance the moistening from the boundary layer below 3 km. Above this level to approximately 7 km convection acts to moisten the atmosphere, which counteracts the drying from the advective forcing. The presence of a tropical low during the suppressed period resulted in dry continental air being advected into the study domain in the midlevels (May et al. 2008). The specific humidity biases in Fig. 9b and 9c show that both of the SCMs produce a significant dry bias in the boundary layer with the diagnostic cloud scheme simulation having a stronger dry bias than the run with PC2. The greater shallow and midlevel convection produced by the diagnostic run during this period (Fig. 4) dries the low levels (Fig. 8c) and results in the stronger moisture bias. The abundant supply of latent heat at these times shown in Figure 1b, forms the moist convective mixing layer that triggers shallow to midlevel convection, which in turn transports the moist boundary layer air to the lower troposphere. The significantly larger than observed latent heat fluxes are predominately due to the strong low level westerly winds of more than 20 m s^{-1} that occurred at these times in the presence of the tropical low. Not enough high cloud and the resulting overestimate of incoming solar radiation at the surface during this period (Fig. 5) could add to the destabilisation of the low levels and be another reason for the overactive convection. This period is the time when the model predicted surface rainfall rates begin to diverge from the observed rates with the models simulating greater precipitation rates. Days 34 - 37 of the experiment were observed to be clear days with no precipitation (see Figs. 2 and 4), however, the models continue to produce surface rainfall though at a reduced rate than the preceding times. The cause of this dry period in the observations was the low specific humidity as shown in Fig. 9a, which neither of the models were able to correctly simulate with the diagnostic cloud scheme simulation resulting in a stronger moist bias.

3.3 The monsoon break period (Julian days 36 - 44)

This is a difficult phase for the SCM to simulate as this regime was characterised by more continental and coastal convection generated from sea breezes resulting in widespread localised convective events. The cloud fraction simulated by the models in the break period, days 35-44, shows more persistent cloud than the observations (Fig. 4), with the simulated cloud fields not penetrating to the same heights as those observed. Throughout the break period the incoming solar radiation at the surface that the models produce is generally in good agreement with the observations even though the OLR is underestimated in this phase of TWP-ICE (Fig. 5). The forcing data for the break period contains the ingredients to produce convection in a SCM, however the resulting cloud fields are overestimated by the models. Given that much of the observed convection during the break period tended to be forced by local scale sea breezes it is not surprising that the simulated cloud properties from a SCM during this phase of the campaign do not tend to compare as well to the observations as the previous phases. The simulated surface precipitation rates during the break period agree well with the observed rain rates, much better in fact that those during the suppressed phase, however the vertical distribution of the cloud fields differs with neither cloud scheme producing deep enough clouds, although PC2 does generate clouds that penetrate about 2 km higher than clouds from the diagnostic scheme.

The temperature increments for the break period in the PC2 simulation shown in Figure 6d result in a net cooling in the levels between 3-15 km with the maximum rate being collocated with the cloud tops. This produces a cold bias at these levels (see Fig. 7a) and is likely to be caused by the overestimate of longwave radiative cooling associated with the excessive cloud produced by the model during this regime. The PC2 simulation has a stronger cold bias than the diagnostic run at the times when there is convection and this is due to greater longwave radiative cooling associated with the greater condensate; PC2 produces 2% less cloud water content and 38% more cloud ice water content over the break period compared to the diagnostic scheme. These increased cloud ice water contents reflect the different ways in which the prognostic cloud scheme interacts with convection. Above the cloud tops the total average temperature increment is a small amount of warming from the shortwave and longwave radiation and this continues the pronounced warm bias that was generated during the suppressed phase as shown in Figure 7a.

The water vapour increments during the break period show a moist bias in the boundary layer (Fig. 8d) but due to the strong dry bias generated by the models during the suppressed period, this moist bias works to reduce the dry bias during the break period. Figure 4 shows that the observations tend to have more cloud top heights at 2-3 km than the models at these times and so while the convection is too active between the heights of 3-6 km, in the levels below this convection is not drying enough.

4. COMPARISON OF CLOUD VARIABILITY BETWEEN THE PROGNOSTIC AND DIAGNOSTIC CLOUD SCHEMES

The temperature and humidity biases shown by the model runs complicate the analysis of model performance. However, they do not obscure a comparison between the fields produced from a prognostic and diagnostic cloud scheme as both of these runs produce similar biases as shown previously. An important distinction between the model runs is the interaction between the convection and the stratiform cloud schemes and interesting insight on these scheme interactions can be obtained by comparing the resulting cloud fields for the TWP-ICE case, which exhibits quite varied convection characteristics throughout the time period.

To explore the variability in the cloud fields that the SCM is able to simulate Figure 10 shows the area cloud fractions plotted as a function of the relative humidity for 4 different heights. The observed relative humidity has been calculated from the observed/analysis temperature and specific humidity fields using the same equations that are used in the model to calculate the saturation mixing ratio. For temperatures above 0°C vapour saturation pressure over water is used and below this temperature the saturation is calculated over ice. Figure 10a shows that at 2 km the relationship between cloud fraction and relative humidity is similar between the models and the observations. PC2 produces more occurrences of cloud fraction below 0.05 than the diagnostic scheme, which is more in line with the observations at this height. The models produce too many clouds with cloud fractions greater than 0.13 and these larger cloud fractions tend to occur at higher relative humidities than they do in the observations. Due to the nature of the PC2 scheme, the result from this simulation shows a wider range of relative humidities where cloud is occurring compared to the diagnostic cloud scheme. At 5km the PC2 simulation produces a greater frequency of cloud fractions below 0.1 than the observations and the diagnostic cloud scheme, with many of these occurring at relative humdities below 40%, which is just below the minimum observed relative humidity that coincides with cloud at this level. The relationship between relative humidity and cloud fractions of 0.1 and greater are comparable between the two model results and the observations at 5 km. The greater variability of cloud fractions with the PC2 scheme has been noted by Wilson et al. (2008b). They also showed that PC2 is able to produce higher cloud fractions in relatively dryer air compared to their control run with the diagnostic cloud scheme, however, in their case this was in better agreement with some stratocumulus observations.

Figure 10c shows that at 10 km the PC2 scheme produces about the same number of occurrences of cloud fractions below 0.1 as the observations, which is significantly more than from the diagnostic scheme, while also being able to correctly capture the number of high cloud fraction events. At 15 km the SCM produces cloud fractions that are much higher than the observations (Fig. 10d), even though the ice water path distributions are quite similar (not shown). As noted earlier, the reduced sensitivity of the radar is likely to have resulted in lower hydrometeor cover in the observational data and at the higher levels there may be some effects of attenuation adding to an underestimate of the observed cloud cover (see e.g. Jakob et al. 2005). Figures 10c and 10d show that at 10 km and above, the observations and model results produce supersaturation with respect to ice. Supersaturations with respect to ice are commonly observed due to the process of ice crystal nucleation not being activated at low supersaturations (e.g. Heymsfield and Miloshevich 1993). Many models convert supersaturation directly to ice, as is the equivalent treatment for warm-phase microphysics, however, these models tend to produce upper tropospheric dry biases (see e.g. Tompkins et al. 2007). Figure 10d shows that the PC2 scheme produces higher cloud fractions than the diagnostic scheme, which is due to the greater ice water content in the PC2 simulation. At 15 km the average ice water content is 7 times greater in the SCM simulation with PC2 compared to that with the diagnostic cloud scheme and this is predominately due to the larger amounts of detrained condensate in the PC2 simulation.

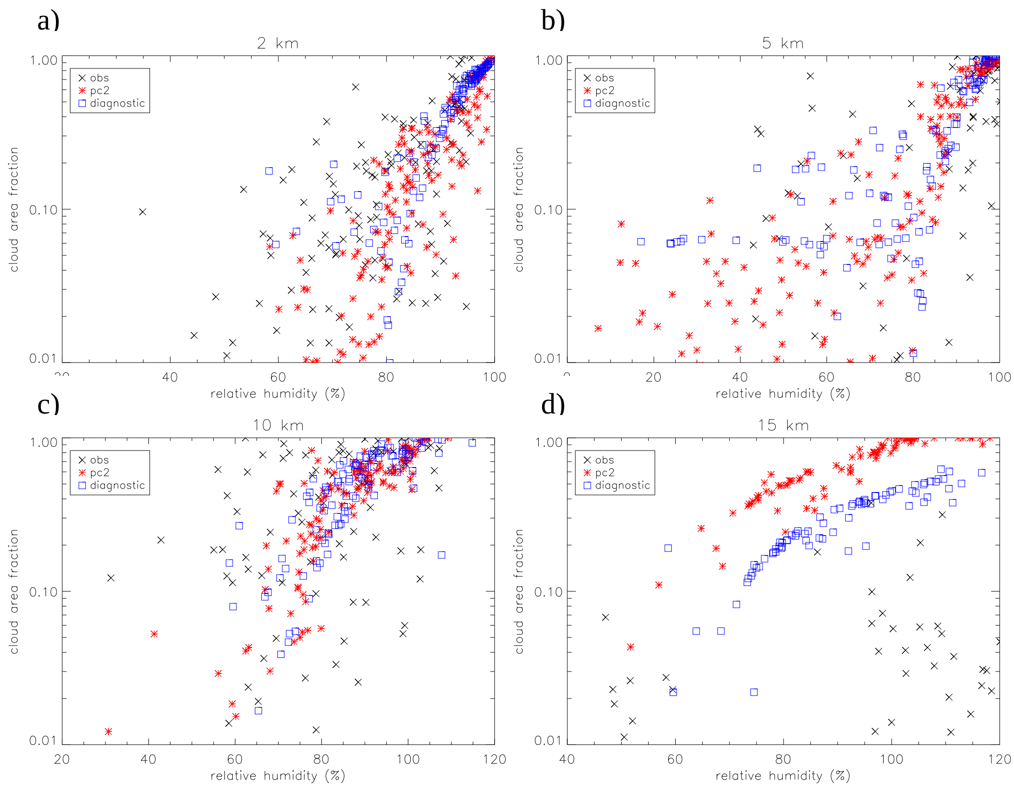

Figure 10: Cloud area fraction plotted as a function of relative humidity for the observations and the 2 SCM runs at the heights of a) 2km, b) 5 km, c) 10 km and d) 15 km.

The process that contributes the most to ice cloud fraction growth in the model is the fall of ice (Wilson and Bushell 2007). This parameterisation in the model determines the amount of overhanging cloud in the layer above and is a function of wind shear. Currently the wind shear is a fixed parameter in the model formulation and a sensitivity test was conducted using the observed wind shear in place of the fixed value of $1.5\times10^{-4}\,s^{-1}$. At times during the simulation the observed wind shear in the anvil cloud is two orders of magnitude larger than the fixed parameter, however, there was no significant effect of using the observed wind shear on the ice cloud fraction for this SCM case.

The vertical distribution of clouds, along with the total cloud amount and optical properties, determines the energy budget of the atmospheric column. The observations of the cloud vertical distribution at the main ARM site in Darwin show a trimodal structure with peaks at 900, 550 and 200 hPa (about 1, 4.5 and 12 km heights) as shown in Figure 11. The SCM vertical cloud distributions have peaks at similar heights to the observations, however the magnitudes of the simulated average cloud cover peaks are greater. The lowest peak in the models and observations is from shallow boundary layer clouds, the peak around 550 hPa is due to the increased stability near the freezing level and the highest peak, which occurs around 12 km, is from anvil clouds developed from the outflow of deep convection. The SCM cloud fractions are larger than the observations throughout all levels of the atmosphere except at the lowest level between the surface and 950 hPa and the region between 600 and 700 hPa. Less midlevel cloud cover is a well known shortcoming of GCMs that occurs in deep convective cloud due to a lack of detrainment from the cumulus parameterisation at these levels, and was documented in a recent study of the global forecast UM by Bodas-Salcedo et al. (2008). For the TWP-ICE case the lack of midlevel cloud from deep convection in the model is partly hidden by the overestimate of midlevel cloud during the suppressed monsoon phase as discussed in section 3.2.

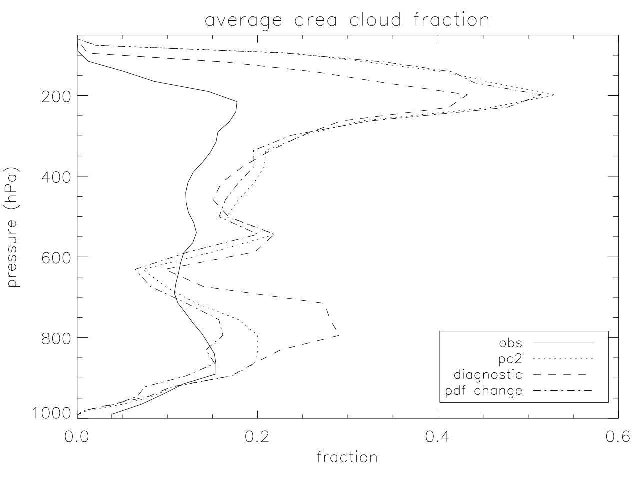

Figure 11: Average cloud area fraction over all times.

Both simulations overestimate the shallow cloud cover, much more so for the model with the diagnostic cloud scheme, which is also shown in Figure 4. The average simulated cloud cover is similar between the two runs from 600 to 250 hPa. The increase in anvil cloud in the PC2 run is due to less condensate being precipitated out of the convective plume and more detrainment into the large-scale cloud due to a change in the convective precipitation function. The overestimation of the high cloud cover from the models may partly be due to the underestimation of the observations at these heights. This is due to the insensitivity of the radar in seeing the small ice particles of the optically thin anvil clouds and the problems with the lidar detecting high cloud when optically thick clouds and precipitation are present below the high cloud (Comstock et al. 2002). How much of the overestimation of the high cloud in the models is due to the limitations of the observations is unknown, however, it seems that while the ice water paths of the models are in fairly good agreement with the observations (not shown), particularly for the PC2 run, the cloud area fractions are to some extent too high.

To investigate the sensitivity of the model clouds to the shape of the distribution of vapour that is used in the closure of the uniform forcing in PC2, a sensitivity experiment was undertaken where the shape of the PDF was changed from a top-hat-like distribution to a triangular distribution (for details on the closure see Wilson and Gregory 2003). The PDF shape is also used in the initiation of cloud in PC2, except for the initiation of cloud from convection or advection (Wilson et al. 2008a). The average cloud area fraction for the sensitivity simulation with the triangular PDF is plotted in Figure 11. For levels above 350 hPa there is very little difference in the cloud cover. In the levels below this the use of a triangular PDF reduces the cloud area fraction, with the greatest change occurring below 750 hPa. The peak in the low cloud cover agrees better with the observations for this simulation where the top-hat PDF shape was replaced by a triangular shape. The greater sensitivity of the low clouds to the change in the PDF is due to the upper clouds being generated and dissipated by deep and midlevel convection and microphysics processes. The microphysics terms have no explicit dependence on the PDF shape and from the result shown in Figure 11 there is a relatively small sensitivity in the model to the specification of the PDF shape in the calculation of the convection cloud fraction changes. The forcing of the low clouds have a contribution from the boundary layer and radiation schemes, which use the homogeneous/uniform forcing of PC2 (Wilson et al. 2008a) and as such depend on the shape of the PDF. Note that the contribution of radiative forcing to the high clouds is through the deposition/sublimation of the microphysics scheme in the model and thus does not use any information on the PDF shape. A further sensitivity test was performed to examine the sensitivity of the PC2 simulation to changes in the phase change temperature between liquid and ice condensate in the convective updrafts. When this temperature is increased from -10°C to the same value that is used in the diagnostic scheme of 0°C the resulting average area cloud fraction shows very little change, except in the region between 450 and 350 hPa where the cloud cover is reduced by about 0.02 (not shown).

To evaluate the distribution of the cloud fields that the SCMs produce, normalised histograms of the cloud area fraction as a function of height have been plotted in Figure 12a for the observations and 12b and 12c for the SCM runs. The observations show that the boundary layer clouds predominately occur with cloud fractions less than 0.25. At these low levels the SCM run with the PC2 cloud scheme looks similar to the observations, however, this model produces no boundary layer clouds with cloud fractions of 1.0 but rather produces more cloud fractions at this height between 0.4 and 0.6 than the observations show. The SCM run with the diagnostic cloud scheme shows a quite different distribution of the cloud cover compared to the observations and the PC2 run. There is less clear sky in the levels below 600 hPa and the cloud fractions from the diagnostic scheme do not change as much with height as the observations and the PC2 results. Both of the SCM runs show many more incidences of high clouds with cloud fractions greater than 0.4 than is present in the observational dataset, with the models simulating very little high cloud with cloud fractions less than 0.3. The simulation with PC2 produces cloud fractions of close to 1 in over 5% of occurrence at the heights above 200 hPa, whereas the observations show no high cloud fractions at these heights.

The cloud area fraction or cloud cover is not the prognostic variable in the PC2 scheme, instead it is the cloud volume fraction. To account for clouds not filling the gridbox in the vertical the ACCESS model uses the diagnostic parameterisation of Brooks et al. (2005) to calculate the cloud area fraction. The Brooks parameterisation is applied to all non-convective clouds. To be consistent, the SCM run with the diagnostic cloud scheme also uses the Brooks method to determine the cloud area fraction. Figures 12d and 12e show the distribution of the cloud

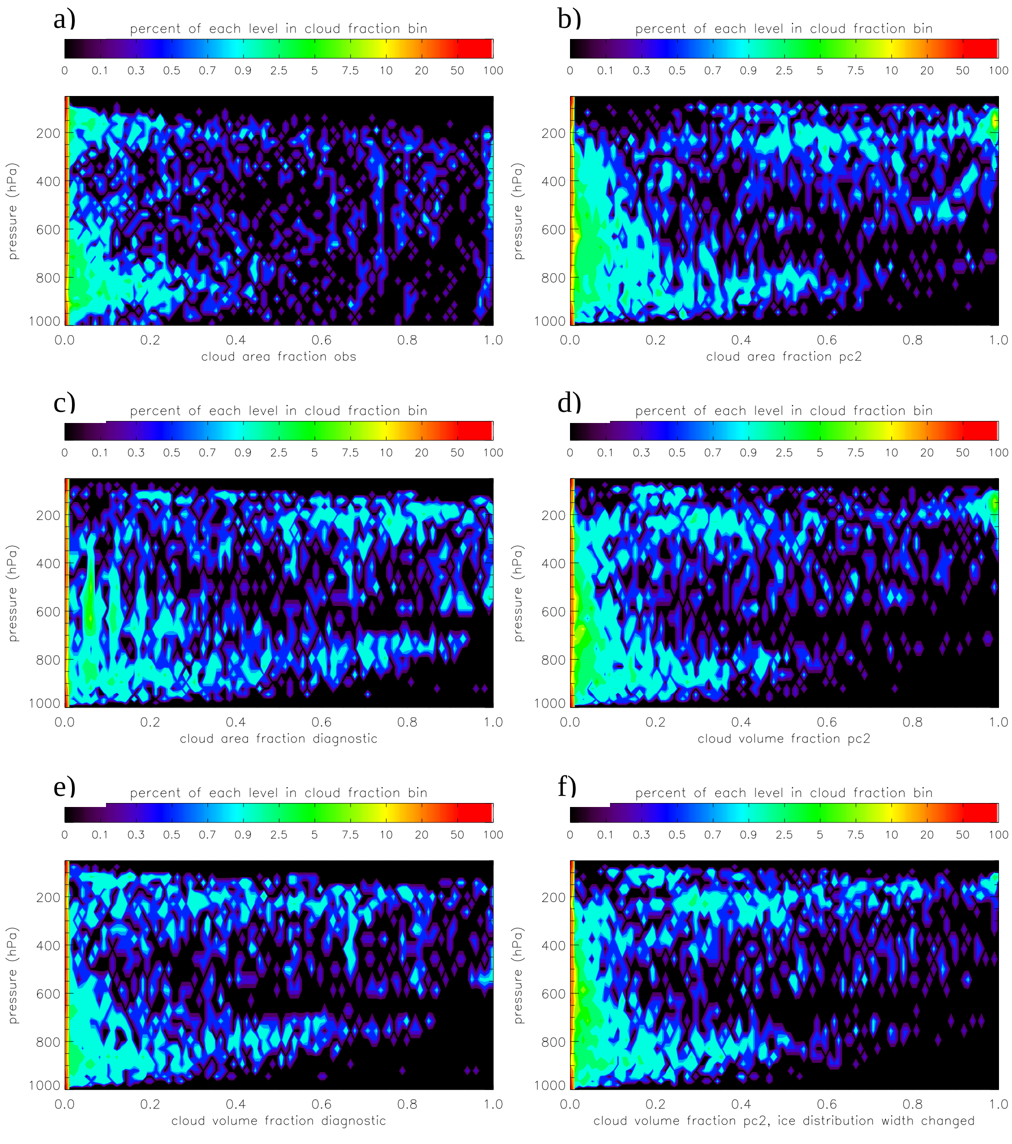

Figure 12: a) Normalised histogram of the observed cloud area fraction as a function of height, b) as for a) except for the SCM results for the PC2 scheme, c) as for a) except for the SCM results for the diagnostic cloud scheme, d) as for b) except for the cloud volume fraction for the PC2 run, e) as for d) except for the cloud volume fraction for the diagnostic scheme run, and f) as for d) except for a change in the ice width distribution (see text for details).

volume fraction for the PC2 and the diagnostic cloud scheme respectively. These distributions generally look more similar to the observations shown in Figure 12a. One can see through the comparison of Figures 12b and 12d and Figures 12c and 12e that the effect of applying the Brooks et al. (2005) scheme is to increase the cloud fractions particularly in the higher levels. The Brooks parameterisation is based on radar and lidar observations from Chilbolton in southern England where the predominant cloud types are stratiform and frontal clouds. Depending on grid box size the cloud area fraction from the parameterisation applied over the observational domain in England was between 20 and 100% greater than the cloud volume fraction (Brooks et al. 2005). The SCM TWP-ICE results in Figure 12 show that applying the Brooks parameterisation to tropical conditions results in an overestimation of the cloud area fraction, at times the cloud volume fraction is increased by 300%.

To calculate the deposition/sublimation of the ice cloud, PC2 includes a parameterisation of the effect that these processes have on reducing the width of the PDF of water vapour fluctuations across the liquid-free portion of the gridbox. Wilson and Bushell (2007) describe this parameterisation and note that it is a linear function of the fraction of mean ice water mixing ratio to the saturation mixing ration, and is tunable by a parameter that is set to 0.04 and multiplies the saturation mixing ratio in this fraction. The result for the distribution of cloud volume fraction from a simulation where this factor is increased to 0.16 is shown in Figure 12f. Comparing Figures 12d and 12f show that by changing this factor, which results in an increase in the width of this PDF, the high cloud fractions reduce from occurring predominately with a value close to 1 to being spread more evenly between 0 and 1. The maximum high cloud area coverage in this simulation reduces by 20% and the amount of ice water condensate reduces by 30%.

A further sensitivity test was performed to see how much difference results in the cloud and radiation fields when no cloud area fraction parameterisation is used in the SCM. In this simulation the cloud area fraction is set equal to the cloud volume fraction predicted by the PC2 scheme and the resulting OLR and incoming solar radiation at the surface are shown in Figure 5. By not applying the Brooks scheme the OLR is generally in better agreement with the observations except during times of the suppressed monsoon phase. The better agreement for the sensitivity run at the times of deep convection stems from the fact that the convection is too persistent and produces too much cloud in the PC2 SCM runs. Hence by not increasing the cloud area fraction in the sensitivity run the result is in better agreement with the observed OLR, except during the suppressed period when the PC2 scheme does not produce enough cloud. The same result is shown in Fig. 5b where the incoming solar radiation at the surface tends to agree better with observations from the PC2 simulation that did not use the Brooks scheme.

5. CONCLUSIONS

The ACCESS SCM, which is the UM SCM of the UK Met Office, has been run for the TWP-ICE case to investigate the ability of the model to represent the vertical distribution and temporal evolution of tropical cloud systems. This SCM study is the first to use the TWP-ICE forcing and evaluation data set and has shown that this case is interesting and useful for model evaluation and development due to the varying nature of the convection during the experiment and the extensive observational dataset. Two SCM runs have been analysed each using a different representation of clouds. A new prognostic cloud scheme, PC2, has been developed at the UK Met Office to overcome some of the problems associated with the tightly constrained cloud fields that are produced by the diagnostic scheme used in the UM. The ACCESS SCM produced generally reasonable representations of the TWP-ICE cloud fields, with the three different observed cloud regimes captured by the model.

The PC2 scheme produced deeper clouds during the active monsoon phase than the diagnostic scheme with 21 and 34% more cloud liquid and ice water condensate respectively, however both models simulated too much total cloud as was shown in the lower values of outgoing long wave radiation. The excessive cloud produced a cold bias in the levels between 7 and 15 km that was due to longwave radiative cooling. Both of the model runs dissipate cloud too soon after the mesoscale convective system event that occurred during the active period, more so for the diagnostic cloud scheme and this produces too much downwelling solar radiation at the surface for the initial times of the suppressed monsoon phase. SCM runs using both cloud schemes failed to maintain a thick enough anvil cloud during the suppressed phase resulting in too little radiative cooling and a warm bias at the heights of the anvil cloud. The final regime in TWP-ICE was the break period and while the observations during this time had many convective events occurring, these systems were smaller in scale than in the active period and characteristic of continental and coastal convection forced by sea breezes. Due to the nature of these convective cells the forcing data contain the ingredients to produce convection in the SCM. However, the model cloud fields are much longer lived than the observed clouds but not as deep. The break period of the experiment is less useful for model evaluation than the other phases because of the difficulties of the SCM to generate representative convection. The greater cloud amounts from the models during the break period produced large longwave radiative cooling in the levels collocated with the thick clouds. The PC2 run showed a stronger cool bias in the upper levels of the clouds during the break period due to an average 38% greater cloud ice water content compared to the run that used the diagnostic cloud scheme. The reason for the greater cloud ice water contents at all times of the simulation is the direct source of cloud condensate from convection in the PC2 scheme. This difference in the way the prognostic and diagnostic cloud schemes interact with convection resulted in a better representation of clouds from the diagnostic scheme during the break period, however, the anvil cloud during the suppressed phase, which was developed from the outflow of deep convection from the active period, was shown to be more representative from the PC2 simulation. It was during the suppressed monsoon phase that there was the greatest difference in the averaged ice condensate amounts with the PC2 simulation producing 67% more than the diagnostic scheme.

The prognostic scheme is able to simulate more variable cloud fields in agreement with the observations as demonstrated by the relationship of cloud fraction with relative humidity. Both model runs were able to produce supersaturation with respect to ice as was observed in the upper levels during TWP-ICE. The lack of midlevel clouds associated with deep convection in the model has been reported by Wilson et al. (2008b) and Bodas-Salcedo (2008) and was exposed in the TWP-ICE results, however, the magnitude of the problem was obscured by the excessive midlevel convection that occurred for both cloud schemes during the suppressed monsoon phase. The frequency distributions of cloud cover as a function of height show that the diagnostic scheme of Brooks et al. (2005) used in the model to convert the cloud volume fraction to the cloud area fraction, overestimates the area cloud fractions at the levels above 12 km. This could be due to the Brooks scheme being developed from observations taken in southern England and the type of stratiform clouds sampled there being quite different to those in tropical conditions. A sensitivity experiment was conducted to test whether a cloud area fraction parameterisation was needed for this case. The results from this simulation showed that without using the Brooks parameterisation OLR tends to be in better agreement with observations at all times except during the suppressed period. This is because in this case at the times of deep convection the SCM overestimates the cloud amount. Further work needs to be undertaken to determine whether a cloud area parameterisation is needed in the model and whether the Brooks et al. (2005) scheme is appropriate for tropical conditions.

Numerous other sensitivity tests were conducted to determine the effects of parameter changes in the cloud and convection schemes on the resulting PC2 simulated clouds. No significant effects were shown when the phase change temperature in the convective plumes was increased from -10 to 0°C and similarly for the simulation where the observed wind shear was included in the formulation for the amount of overhanging cloud used in the calculation of the fall of ice. Significant sensitivity in the PC2 simulated low clouds was demonstrated when the shape of the distribution of water vapour was changed from a top-hat-like shape to a triangular distribution. The reduction that occurred in the low clouds when the triangular PDF was used was in better agreement with the observations. The sensitivity of the low clouds is due to these clouds including the homogeneous forcing (Wilson et al. 2008a) used by the boundary layer and radiation schemes that depend on the shape of the PDF. The high clouds on the other hand are predominately determined by the convection scheme, which does include the PDF shape in the calculation of the convective cloud fraction changes, however, the model shows relatively little sensitivity in this term to the change in PDF shape. The area cloud cover of high clouds was shown to be sensitive to the change in the width of the distribution of vapour fluctuations in the liquid-free portion of the grid box, which is used to determine the amount of deposition/sublimation. When the constant used in this parameterisation was increased by a factor of 4, which resulted in an increase in the width of this PDF, the high cloud cover reduced by 20%. This reduction resulted in about the same average high cloud cover as the diagnostic scheme run and a greater amount of high cloud occurring with cloud fractions between 0.4 and 0.8, rather than too many incidences occurring at cloud fractions close to 1, which is not shown in the observations. Future work will evaluate the impact of these sensitivities in the three-dimensional model.

Lin et al. (2004) suggested that the inability of many models to simulate realistic representations of the MJO may be caused by systematic diabatic heating profile errors. Temperature and moisture errors in the SCM simulations were seen to be the most pronounced during the suppressed and break periods. Other studies such as Li et al. (2008) have identified the link between poor simulations of suppressed convection leading to unrealistic simulations of sub-seasonal variability in tropical convection, including the MJO, and TWP-ICE may provide a good case to study the model biases and make improvements in the model cloud and convection parameterisations. The GEWEX Cloud Systems Study Group (GCSS) is currently setting up a TWP-ICE experiment as an intercomparison case for both SCMs and CRMs. This experiment will use the forcing and evaluation data set that was used in this study and the outcomes from the high resolution models will enable a more rigorous assessment of the link between the cloud scheme and the convection parameterisation in the ACCESS/UM SCM and the ability of the model to simulate tropical cloud system. This is intended to build on the results reported herein and lead to improvements to the physical parameterisations.

6. ACKNOWLEDGEMENTS

CNF was funded by the Australian Department of Climate Change. CNJ is grateful for support from the U.S. Department of Energy under grant DE-FG02-03ER63533 as part of the Atmospheric Radiation Measurement Program. Data were obtained from the Atmospheric Radiation Measurement (ARM) Program sponsored by the U.S. Department of Energy, Office of Science, Office of Biological and Environmental Research, Environmental Sciences Division. The forcing data were generated by Shaocheng Xie from the Lawrence Livermore National Laboratory. CNF would like to acknowledge Dr Damian Wilson from the Met Office for discussions and insight on PC2 and Drs Jon Petch from the Met Office and Tim Hume from the Centre for Australian Weather and Climate Research (CAWCR) for discussions on the TWP-ICE forcing data. Drs Peter May and Leon Rotstayn (CAWCR) are thanked for providing helpful comments on the manuscript.

REFERENCES

Bechtold, P., Redelsperger, J.L., Beau, I., Blackburn, M., Brinkop, S., Grandpeix, J.Y., Grant, A., Gregory, D., Guichard, F., Hoff, C. and Ioannidou, E. 2000. A GCSS model intercomparison for a tropical squall line observed during TOGA-COARE. Part II: Intercomparison of single column models and a cloud resolving model. *Q. J. R. Meteorol. Soc.,126,* 865-888.

Bergman, J.W. and Sardeshmukh, P.D. 2003. Usefulness of single column model diagnosis through short-term predictions. *J. Climate, 16,* 3803-3819.

Bodas-Salcedo, A., Webb, M.J., Brooks, M.E., Ringer, M.A., Williams, K.D., Milton, S.F. and Wilson, D.R. 2008. Evaluating cloud systems in the Met Office global forecast model using simulated CloudSat radar reflectivities. *J. Geophys. Res., 113,* doi:10.1029/2007JD009620.

Brooks, M.E., Hogan, R.J. and Illingworth, A.J. 2005. Parameterizing the difference in cloud fraction defined by area and by volume as observed with radar and lidar. *J. Atmos. Sci., 62,* 2248-2260.

Clothiaux, E.E., Ackerman, T.P., Mace, G.G., Moran, K.P., Marchand, R.T., Miller, M.A. and Martner, B.E. 2000. Objective determination of cloud heights and radar reflectivities using a combination of active remote sensors at the ARM CART sites. *J. Appl. Meteor., 39*, 645-665.

Comstock, J.M., Ackerman, T.P. and Mace, G.G. 2002. Ground-based lidar and radar remotesensing of tropical cirrus clouds at Nauru Island: Cloud statistics and radiative impacts. *J. Geophys. Res., 97,* 3831-3836.

Davies, T., Cullen, M., Malcolm, A., Mawson, M., Staniforth, A., White, A.A. and Wood, N. 2005. A new dynamical core for the Met Office's global and regional modelling of the atmosphere. *Q. J. R. Meteorol. Soc., 131*, 1759-1782.

Edwards, J.M. and Slingo, A. 1996. Studies with a flexible new radiation code. I: Choosing a configuration for a large-scale model. *Q. J. R. Meteorol. Soc., 122*, 689-719.

Fridlind, A.M, Ackerman, A.S., Petch, J., Jakob, C. and Xie, S., 2008. Monsoonal deep convection during TWP-ICE/ACTIVE: Progress on an idealized 6 day case study. Abstracts of thttp://www.knmi.nl/~siebesma/PAN-GCSS/

Ghan, S.J., Leung, L.R. and McCaa, J. 1999. A comparison of three different modelling strategies for evaluating cloud and radiation parameterizations. *Mon. Wea. Rev., 127*, 1967-1984.

Gregory, D. and Rowntree, P.R. 1990. A mass flux convection scheme with representation of cloud ensemble characteristics and stability-dependent closure. *Mon. Wea. Rev., 118*, 1483-1506.

Heymsfield, A.J. and Miloshevich, L.M. 1993. Homogeneous ice nucleation and supercooled liquid water in orographic wave clouds. *J. Atmos. Sci., 50,* 2335-2353.

Hume, T. 2007. Radiation dry bias in the TWP_ICE radiosonde soundings. *The 17th ARM Science Team Meeting*, California, USA. Available from http://www.arm.gov/publications/proceedings/conf17/index.php

Jakob, C., Tselioudis, G., and Hume, T. 2005. The radiative, cloud, and thermodynamic properties of the major tropical western Pacific cloud regimes. *J. Climate, 18*, 1203-1215.

Li, C., Jia, X., Ling, J., Zhou, W. and Zhang, C. 2008. Sensitivity of MJO simulations to diabatic heating profiles. *Clim. Dynam.,* doi 10.1007/s00382-008-0455-x

Lin, J.-L., Mapes, B., Zhang, M. and Newman, M. 2004. Stratiform precipitation, vertical heating profiles and the Madden-Julian oscillation. *J. Atmos. Sci., 61,* 296-309.

Lock, A.P., Brown, A.R., Bush, M.R., Martin, G.M. and Smith, R.N.B. 2000. A new boundary layer mixing scheme. Part I: Scheme description and single-column model tests. *Mon. Wea. Rev., 128*, 3187-3199.

May, P.T., Mather, J.H., Vaughan, G., Jakob, C.N., McFarquhar, G.M., Bower, K.N. and Mace, G.G. 2008. The Tropical Warm Pool International Cloud Experiment (TWP-ICE). *Bull. Amer. Meteor. Soc., 89*, 629-645.

Menon, S., Brenguier, J.-L., Boucher, O., Davison, P., Del Genio, A.D., Feichter, J., Ghan, S., Guibert, S., Liu, X., Lohmann, U., Pawlowska, H., Penner, J.E., Quaas, J., Roberts, D.L., Schüller, L. and Snider, J., 2003. Evaluating aerosol/cloud/radiation process parameterizations with single-column models and Second Aerosol Characterization Experiment (ACE-2) cloudy column observations. *J. Geophys. Res., 108,* doi:10.1029/2003JD003902.

Menon, S. and Rotstayn, L., 2006: The radiative influence of aerosol effects on liquid-phase cumulus and stratiform clouds based on sensitivity studies with two climate models. *Clim. Dynam., 27,* 345-356.

Randall, D.A., Xu, K.-M., Somerville, R.J.C. and Iacobellis, S. 1996. Single-column models and cloud ensemble models as links between observations and climate models. *J. Climate,* **9**, 1683-1697.

Roe, P.L. 1985. Large scale computations in fluid mechanics. *Lectures in Applied Maths, 22,* No.2 Berlin: Springer pp 163-193.

Smith, R.N.B. 1990. A scheme for predicting layer clouds and their water contents in a general circulation model. *Q. J. R. Meteorol. Soc., 116,* 435-460.

Tiedtke, M. 1993. Representation of clouds in large-scale models. *Mon. Wea. Rev., 121*, 3040-3061.

Tompkins, A.M., Gierens, K. and G. Rädel 2007. Ice supersaturation in the ECMWF integrated forecast system. *Q. J. R. Meteorol. Soc., 133*, 53-63.

Wilson, D.R. and Ballard, S.P. 1999. A microphysically based precipitation scheme for the Meteorological Office Unified Model. *Q. J. R. Meteorol. Soc., 125*, 1607-1636.

Wilson, D. and Gregory, D. 2003. The behaviour of large-scale model cloud schemes under idealized forcing scenarios. *Q. J. R. Meteorol. Soc., 129*, 967-986.

Wilson, D., Smith, R.N.B., Gregory, D., Wilson, C., Bushell, A.C. and Cusack, S. 2004. Unified Model documentation paper 26. The large-scale cloud scheme and saturated specific humidity. Available from Met Office.

Wilson, D. and Bushell, A. 2007. Annexe to Unified Model documentation paper 29. The PC2 cloud scheme. Available from Met Office.

Wilson, D.R., Bushell, A.C., Kerr-Munslow, A.M., Price, D. and Morcrette, C. 2008a. PC2: A prognostic cloud fraction and condensation scheme. Part I: Scheme description. *Q. J. R. Meteorol. Soc.*, in press.

Wilson, D.R., Bushell, A.C., Kerr-Munslow, A.M., Price, D., Morcrette, C. and Bodas-Salcedo, A. 2008b. PC2: A prognostic cloud fraction and condensation scheme. Part II: Results of climate model simulations. *Q. J. R. Meteorol. Soc.*, in press.

Xie et al. 2007. Objective Variational Analysis for the Tropical Warm Pool International Cloud Experiment. *The 17th ARM Science Team Meeting,* California, USA. Available from http://www.arm.gov/publications/proceedings/conf17/index.php

Zhang, M.H. and Lin, J.L. 1997. Constrained variational analysis of sounding data based on column-integrated budgets of mass, heat, moisture and momentum: Approach and application to ARM measurements. *J. Atmos. Sci., 54*, 1503-1524.

Zhang, M.H., Lin, J.L., Cederwall, R.T., Yio, J.J. and Xie, S.C. 2001. Objective analysis of ARM IOP data: Method and sensitivity. *Mon. Wea. Rev.,129*, 295-311.

The Centre for Australian Weather and Climate Research is a partnership between CSIRO and the Bureau of Meteorology.